Journal of Azzaytuna University (JAZU)
JAZU Homepage: https://azzujournal.azu.edu.ly
ISSN (Print):2523-1006, ISSN (Online): 3105-4420 DOI: 10.35778/jazu.i56.a679

A Compact Transparent Dual-Element Antenna with Improved Isolation

Abdulati I. Abdullah[1,*], fuad E. F. Mohammed [2], Ahmed H Elshoshi[3], Abubaker M Algatlawi[4] and Yousef A. A. Hammad [5]

[1,2] Department of Electric Engineering, Faculty of Engineering, Azzaytuna University , Tarhunah, Libya
[3]Department of Electric Engineering, Higher Institute of Engineering Technology, Tripoli, Libya
[4,5]Department of Electric Engineering, Higher Institute of Science and Technology, Tarhunah, Libya
[1]a.abdullah@azu.edu.ly, [2]fuademran88@gmail.com, [3]a.elshoshi@hiett.edu.ly, [4] aljetlawi10203040@gmail.com, [5]hammadyousf577@gmail.com

Corresponding Author (*)

Publishing Date: 31 December 2025

ABSTRACT: **A mm-wave wideband compact transparent antenna is designed on Plexiglas substrate with dimension of 10.235x10x0.508 mm^3 and then the ground plane is modified resulting in bandwidth enhancement. The proposed antenna achieves a bandwidth of 13.5 GHz and supporting two resonant frequencies at 24.7 GHz and 33.8 GHz with return losses of -35dB, and -33dB and gain of 6.4dB and 4.5dB respectively, in addition to achievable efficiency reaches up to 85%. The design is extended to two antenna elements with inverted U-slab shaped as a parasitic element introduced between antennas used for improving isolation and therefore reduce the mutual coupling. The separation between two elements is less than $\lambda/2$ resulting in isolation less than -39 dB with ECC is about 0.002 and diversity gain (DG) of 10 at the resonant frequency of 25.561 GHz to support 6 GHz of operating bandwidth. This result demonstrates a considerable improvement in antenna compactness, properties, and spectral efficiency; thereby it can be an excellent candidate to be used for 5G wideband applications and beyond.**

Keywords: **Transparent antenna, Plexiglas, Mutual coupling, ECC, DG, 5G**

الملخص: تم تصميم هوائي شفاف مدمج واسع النطاق يعمل في نطاق الموجات المليمترية (mm-wave) على ركيزة من مادة الـ Plexiglasبأبعاد 0.508 × 10 × 10.235مم^3، ثم جرى تعديل مستوى التأريض مما أدى إلى تعزيز عرض الحزمة. يحقق الهوائي المقترح عرض حزمة قدره 13.5جيجاهرتز، ويدعم ترددين رنينيين عند 24.7جيجاهرتز و 33.8جيجاهرتز مع معاملات انعكاس بلغت 35-ديسيبل و 33-ديسيبل على التوالي، وكسب مقداره 6.4ديسيبل و 4.5ديسيبل، إضافةً إلى كفاءة تشغيلية تصل إلى .85% تم تطوير التصميم ليشمل عنصرين هوائيين، مع إدخال عنصر طفيلي على شكل لوح مقلوب على هيئة Uبين الهوائيين، وذلك لتحسين العزل وتقليل الاقتران المتبادل. كانت المسافة الفاصلة بين العنصرين أقل من λ/2، مما أدى إلى تحقيق عزل أقل من 39-ديسيبل، ومعامل ارتباط مغلف (ECC) يقارب 0.002، وكسب تنوعي (DG) يساوي 10عند التردد الرنيني 25.561جيجاهرتز، لدعم عرض حزمة تشغيلية يبلغ 6جيجاهرتز. تُظهر هذه النتائج تحسناً ملحوظاً في مدمجية الهوائي، وخصائصه الكهرومغناطيسية، وكفاءته الطيفية، مما يجعله مرشحاً ممتازاً للاستخدام في تطبيقات الاتصالات واسعة النطاق للجيل الخامس (5G)وما بعدها.

الكلمات المفتاحية: الهوائي الشفاف، (Plexiglas)، الاقتران المتبادل، معامل الارتباط المغلف(ECC) ، الكسب التنوعي (DG)، الجيل الخامس.(5G)

I. INTRODUCTION

A considerable development in mobile communications technology is often linked to the evolution of materials and devices that are manufactured for the purpose of transmitting and receiving signals or data [1]. Therefore, the evolution of 5G and beyond in the field of wireless communication has multiplied the amount of data transferred to users by many times compared to the fourth generation [1], [2]. As the 5G supports delivering a massive data rate, the performance of the system becomes much better in terms of seamless

connectivity, and ultra-low latency, smoother in data streaming and download speed than previous generations [3]. All these features help to improve the performance further and play a fundamental role in the emergent of the technologies as autonomous vehicles and IoT. Generally, it is stated that each generation has the potential to be revolutionary [2] , such as, in 5G, which is founded to achieve data rate of 20 Gbps in the normal conditions with lower latency of less than 1ms, which is massive development compared to 1Gbps that is delivered by 4G LTE with latency reported between 20 and 50 ms. In a particular scenario, millimiter wave (mm-wave) spectrum in 5G supports data transmission of several Gbps in metropolitan areas with a frequency band spanning from 24.25 GHz to 52.6 GHz, where a dense of base stations are mounted to cover the small areas and therefore enhancing the data transmission [4] , [5]. For that case, the essential part of the communication scenario is the wearable electronics context in which some key aspects of design required such as, an antenna working at mm-wave range with a small size, and affectivity to launch the 5G requirements. Therefore, the interest in designing compact antennas in 5G grows continuously taking into account the type of the antenna, cost and circuit complexity [6]. In this paper the optically transparent antenna is designed. The transparent antenna is defined as a class of antennas that sustain an optical transparency with ensuring the performance of an efficient radio frequency. It is designed by deploying a material that allows the visible light to pass through and integrates with the glass surfaces such as on window, and vehicles [7], [8]. The main concerns with choosing the materials for these antennas are transparency, efficiency and conductivity. The main common materials used as a substrate, which are highly transparent, are Indium Tin Oxide (ITO), AgHT-4, AgHT-8 and Plexiglas materials; fluorine doped tin oxide on glass and polyimide. For transparent antenna, as the surface resistance increases, this results in an increase in optical transparency [7], [9]. However, the main challenging parts of designing the transparent antennas are the fabrication of the materials and the antenna efficiency. There is also a trade of between conductivity and transparency, as to achieve high transparency (more that 90%) , the conductive materials should be more thinly than the conventional one, this leads to lower conductivity while increases the sheet resistivity, resulting in reduction in the antenna gain and efficiency [10], [11]. The transparency may be obtained by meshing the conventional conductor, to solve the problem in straightforward way and it becomes simple to construct on windshield or solar cells [12]. In the metropolitan environment, the transparent antennas can be embedded into the glass of high-rise buildings may be deployed as a camouflage antenna to support the connectivity in the uncovered areas, whereas, this can degrade the gain, radiation pattern and efficiency [13].The techniques used to change an opaque antenna to transparent one are inefficient leading to reduction in the performance of the antenna because of the meshing of the conducting element or resistivity of thin films [13]. For the design of transparent antenna, there must have a balance in transparency with conductivity, thereby the choice of the materials is necessary and challengeable. In this case, the substrate on which the conductive material positioned or fabricated must be transparent with conceivable dielectric properties, such as glass or other materials that are mentioned in [14]. Moreover, it is essential to be careful with choosing the conductive transparent materials by considering their transparency, conductivity and applications that this antenna supports.

Although antenna selection and design to meet applications serving a specific frequency band is essential, the modern industries of communications technologies have currently concentrated their design on miniaturization of devices, increasing the spectral efficiency, reducing latency, increasing the throughput and reliability [15]. These key advantages can be obtained using the MIMO (Multiple input- Multiple output) technology, that supports the share of dynamic spectrum to improve the capacity and spectral

efficiency. When MIMO is integrated with transparent antennas, seamless integration is enabled into surface such as, smart windows, automotive glass, etc. Despite its many advantages in modern communication systems, MIMO system suffers from a problem of Mutual coupling (MC) [4]. Mutual coupling appears between closely spaced antenna elements especially when the distance between the neighboring elements is less than the half of the wavelength. The MC causes the performance degradation results in reduction in the isolation and an increase in the correlation between the elements [16]. For more clarity, MC presents in case of the electromagnetic fields produced form one antenna interacts with other neighboring antennas elements in the array. This interaction results in change in the impedance, radiation pattern, and system efficiency, thus the performance in general is degrade [4]. By addressing this problem, the potential solution has been introduced by using effective techniques to suppress or null out the MC effect and achieve the miniaturization property. As without decoupling techniques, compactness of devices becomes challenging due to reduction of bandwidth, lower efficiency and higher MC. However, compactness in antennas is required in modern wireless communications as in 5G and beyond; this needs to an efficient MIMO antennas occupying minimal place in the device [17]. One of the possible techniques for miniaturizations is to use a substrate with higher permittivity, this allows for smaller size of antenna dimensions due to reduction in wavelength. This mechanism causes reduction in bandwidth and efficiency. The most common techniques that have been used as a filter to reduce the mutual coupling are, defected ground structure (DGS), some neutralization lines with various forms etched between active elements as parasitic, frequency selective surfaces FSS, and metamaterials and metasurfaces [18], [19].

The performance of MIMO system is evaluated using different parameters to optimize the system efficiency in the presence of MC. The most important key metric is Envelope Correlation Coefficient (ECC) [20]. It describes the correlation among the signals transmitted or received by multiple antennas. It is expressed in two methods in terms of far-field radiation pattern for an isotropic ideal multipath environment [20], suppose having two antennas, antenna i and antenna j, the ECC between these antennas is expressed as follow.

$$\rho_{ij} = \frac{\left|\iint_{\Omega_1}^{\Omega_2}[F_i(\theta,\varphi).F_j^*(\theta,\varphi)]d\Omega\right|^2}{\iint_{\Omega_1}^{\Omega_2}|F_i(\theta,\varphi)|^2 d\Omega.\iint_{\Omega_1}^{\Omega_2}\left|F_j^*(\theta,\varphi)\right|^2 d\Omega} \quad (1)$$

The second method of expressing the ECC between two antennas elements is S-parameter method, when the distance between two neighboring antennas is closer.

$$\rho_{ij} \approx \frac{\left|S_{ii}^* S_{ij} + S_{ij}^* S_{jj}\right|^2}{(1-|S_{ii}|^2-|S_{ji}|^2)(1-|S_{jj}|^2-|S_{ij}|^2)} \quad (2)$$

The importance of calculating ECC is evaluate the diversity of the gain (DG) , the lower the ECC is the better the diversity, this ensures more reliability of propagated signal in fading conditions of the channel [20], [21].

$$DG = 10.\sqrt{1-\rho_{ij}} \quad (3)$$

The ECC also affect the capacity of MMO system. This is because MIMO system supports the spatial multiplexing, therefore, it is crucial to control the correlation between antennas to be less than 0.3 in practice.

In general, it is desirable to have ECC as less as possible; this can be controlled by either increase the space between the antennas to minimize MC, design antennas support pattern diversity or polarization diversity, or use decoupling structures to suppress the MC [22], [23].

This work aims at designing a compact transparent antenna with DGS and then the design is extended to have two element antennas to investigate the figure of merit in for multiple antennas system.

II. ANTENNA DESIGN

The geometry of the suggested compact transparent antenna is designed as shown in fig. (1-a). it consists of microstrip patch that is inset fed, to achieve better matching between antenna input impedance and the impedance of the transmission line, as the current reaches its maximum at the central of the patch contributes in reducing the impedance effect. The conducting part of the antenna is made of transparent conductive material with electric conductivity of 4.561x 10^7 s/m, and mounted on a transparent substrate with diminutions of 10.235x10x0.508 mm^3 made of Plexiglas with loss tangent and dielectric constant of 0.00037 and 2.2 respectively. For achieving compactness, the ground is modified as shown in fig.(1-b) where the length of the ground plane is modified to a half of the wavelength, then removing a shape of rectangular slot in both sides of the ground plane with a length of quarter- wavelength. The ground plane adjustment offers several advantages as enhancing the shape of the radiation pattern to be more directional, improving the gain, and impedance matching. It supports broadband performance providing a wider bandwidth, to have suitability for the proposed antenna to function with broader frequencies range. Therefore, modifying the ground plane allows compactness of the design for limited spaces.

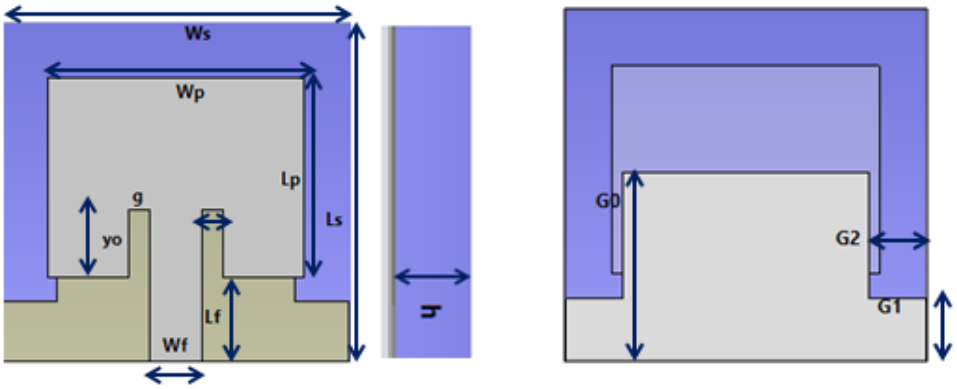

Top-views , and thickness of substrate Bottom view

Fig. 1. Proposed antenna structure.

The surface resistivity (R_σ) of the transparent conductive material is calculated to figure out the electric characteristics of the materials where the current can flow along. The R_σ is expressed in Ω for each square regarding less the conductive material size and calculated as follows:

$$R_\sigma = \frac{\rho}{t} \qquad (4)$$

Where, ρ is the Bulk resistivity measured in $(\Omega.m)$, and t is the thickness of the conductive materials measured in (m).

The transparent antenna in this article is design using CST microwave studio, with dimensions are set by using the equations of designing the microstrip patch antenna as shown in [24] , where the length, width of patch can be calculated, and width and length of substrate accordingly. The width of the microstrip line is crucial for impedance matching and minimizing signal reflections. Thus, it is important to determine the width of the feeding line by selecting the desirable characteristic impedance Z_o, the dielectric constant and thickness of the substrate, and the thickness of the conducting patch which is the same as that for feeding line as shown in equation (5) [24].

$$z_0 = \frac{87}{\sqrt{\varepsilon_r + 1.41}} \ln\left(\frac{5.98\,(h)}{0.8\,w_f + t}\right) \qquad (5)$$

Where: Z_o is the characteristic impedance and commonly sets to 50 Ω, ε_r is the dielectric constant of the substrate, h is the substrate thickness in (mm), which is reasonably chosen in the range between $0.003\lambda_0$ and $0.05\lambda_0$, where λ_0 is the wavelength calculated in free space, w_f is the width of the feeding line and t is the conducting patch thickness. There is another method to find out the width of the feeding line is by using the simulation tools as shown in fig. (2), in this window, after defining the frequency, thicknesses of substrate and conducting patch, feeding length and dielectric permittivity, w_f will be changed till achieve $z_0 = 50\Omega$.

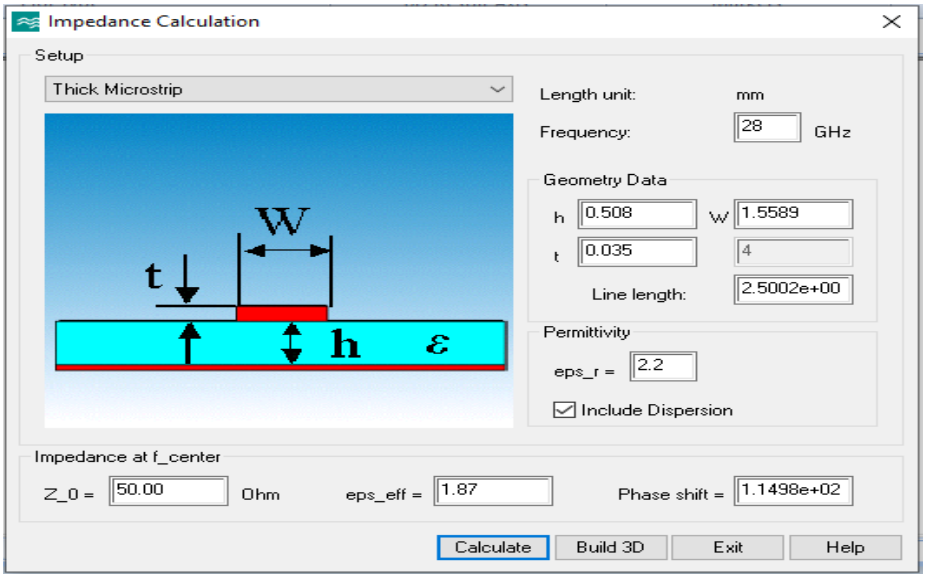

Fig. 2. Impedance calculations window in CST MW Studio

The patch is design as inset fed, in order to reduce the effect of the input impedance; this can be calculated as in the following equation [24].

$$y_0 = \frac{L_p}{\pi} \cos^{-1}\left(\frac{z_0}{R_{in}}\right) \qquad (6)$$

Where y_0 is the position of inset fed, and R_{in} is the measured resistance at the edge of the patch and known as resonant impedance. It is typically large form 100-150Ω. This impedance can be calculated as follows:

$$R_{in} \approx 90\left(\frac{\varepsilon_r}{\varepsilon_r+1}\right)\left(\frac{L_p}{W_p}\right) \quad (7)$$

III. RESULTS AND DISCUSSIONS

A. Results of the design with full ground

The proposed antenna is initially designed based on the mathematical procedure of microstrip patch antenna with full conductive ground plane. The designated equations are presented in details in [24] where the length and width of patch, and width and length of the Microstrip feeding line and thickness of the substrate can be calculated. Table (1) demonstrates the initial dimensions of the antenna parameters obtained by using the equations of the design. The resonant frequency used is 28GHz, which is commonly used in the 5G applications in order to achieve the compactness property.

Table 1 Parameters dimensions of the antenna design

No	Parameter	Dimensions (mm)
1	Width of Patch (w_p)	7.6
2	Length of Patch (L_p)	5.9
3	Thickness of Substrate (h)	0.508
4	Width of Substrate (w_s)	10.235
5	Length of Substrate (L_s)	10
6	Width of feeder (w_f)	1.578
7	Length of feeder (L_f)	2.5
8	Length of inset (yo)	2
9	Width of inset (G)	0.1

Fig. 3, shows the return loss (S_{11}-parameter) for the full ground design, the figure explains the results obtained by changing the dimension of patch length (L_p), as there is an inverse proportional relation between the patch length and the resonant frequency. In this deign three values are set for patch length to get closer to the desirable resonant frequency of 28GHz, for Lp with 5 mm the resonant frequency obtained at about 28GHz with return loss (S_{11}) of nearly -43 dB. The importance of considering the return loss to be less than -10dB is that because S_{11} measures the power loss due to its refection toward an unwanted direction because of the impedance mismatching between the feeder and antenna at the feeding point. For $S_{11} < -10\ dB$, it is widely used as an accepted standard for well matching of the antenna to efficiently deliver power by ensuring more than 90% of the power is delivered in the desirable direction. The following equations demonstrate how to calculate the reflected and delivered power toward free space.

$$S_{11} = 10\ log_{10}\ |\Gamma|^2 \quad (8)$$

Where Γ represents the reflection coefficient, $|\Gamma|^2$ represents the reflected power and (1- $|\Gamma|^2$) represents the power accepted by the antenna. In this deign the minimum return loss is achieved at 28GHz with

approximately $S_{11} = -43$ dB, this results in 0.00005 of the power is reflected with a percentage of 0.005% form the total power, while 99.99% is delivered.

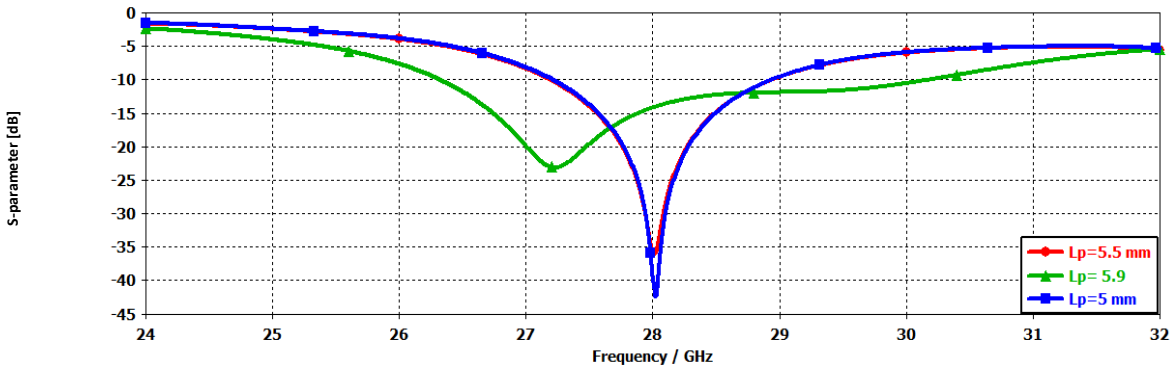

Fig. 3. Simulated S_{11} for the proposed antenna with full ground plane

For the $S_{11} = -43dB$, the antenna provides a bandwidth of approximately 1.8 GHz, with impedance bandwidth of 6.43%. At such resonant frequency, the voltage standing wave ratio (VSWR) gets 1.02, which is closer to the minimum reference of VSWR accepted value $(1 \leq VSWR \leq 2)$.

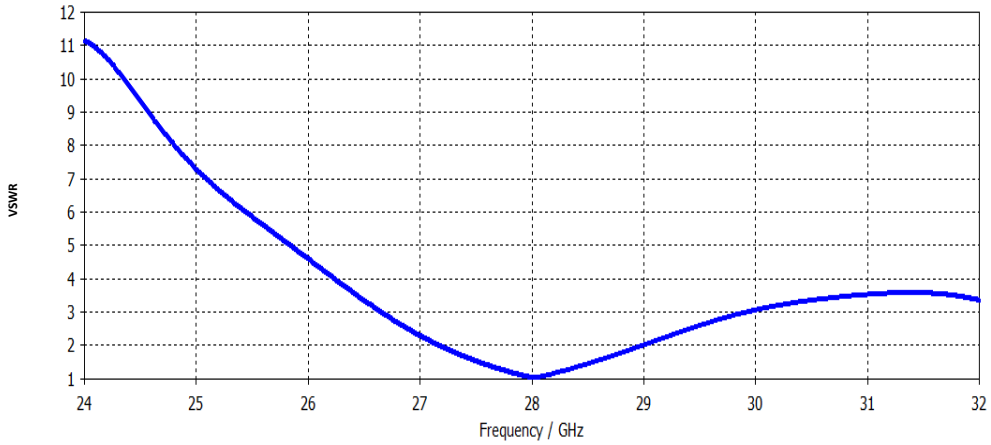

Fig. 4 .Simulated VSWR for the proposed antenna

Fig.5, shows the radiation pattern of the proposed design at 28 GHz, the radiation exhibits a more directional in E-plane at $(\theta = 0^0)$, and an omnidirectional in H-plane at $(\theta = 90^0)$ which more suitable for the 5 G or mm-wave applications

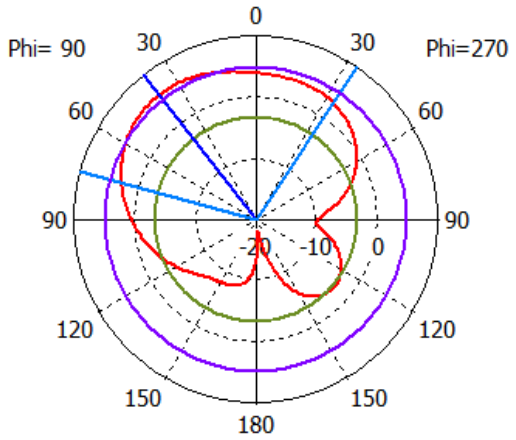

Fig.5. Far-field radiation pattern of at 28GHz

The essential key parameter of measuring the antenna performance is the radiation efficiency, as it is defined as the ratio of the power reflected back to the total input power supplied by the source. It basically quantifies the capability of the antenna to convert the input power to be radiated as electromagnetic waves. It considers the losses result from conduction and dielectric materials that can absorb the energy, and surface waves due to power trapped in antenna substrate, as well as losses due antenna mismatching. For improving the radiation efficiency, it is required to optimize the thickness of the substrate 'h'. The significance of choosing a proper value 'h' is due to its effect on the bandwidth and the radiation efficiency, therefore the thicker the thickness is the wider the bandwidth but it reduces the radiation efficiency due to an increase in excitation of surface waves and thereby the losses increases. In addition, using defecated ground structure (DGS) or parasitic slot as decoupling techniques will improve the efficiency of the system by suppressing the surface waves. In this design the substrate thickness is set at 0.508 mm to provide an antenna efficiency of about 85% in the bandwidth range where the antenna can operate as illustrated in fig.6 . This result in antenna gain is closer to 6.5 dB at resonant frequency of 28GHz as shown in fig.7.

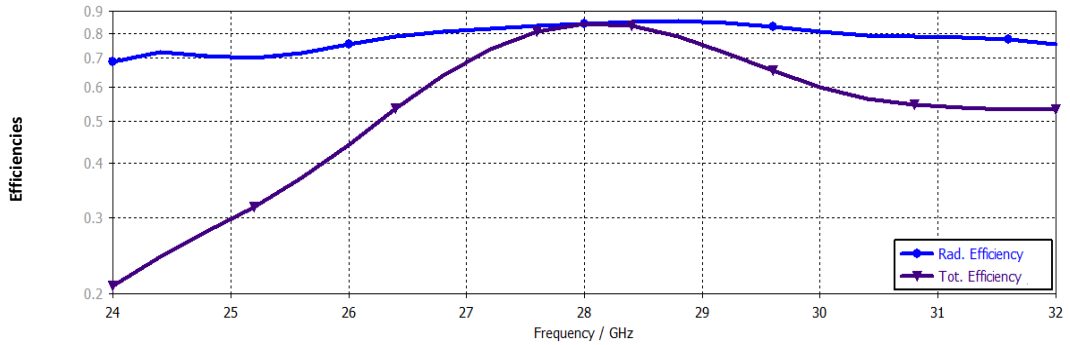

Fig.6. Radiated and total efficiency of the design

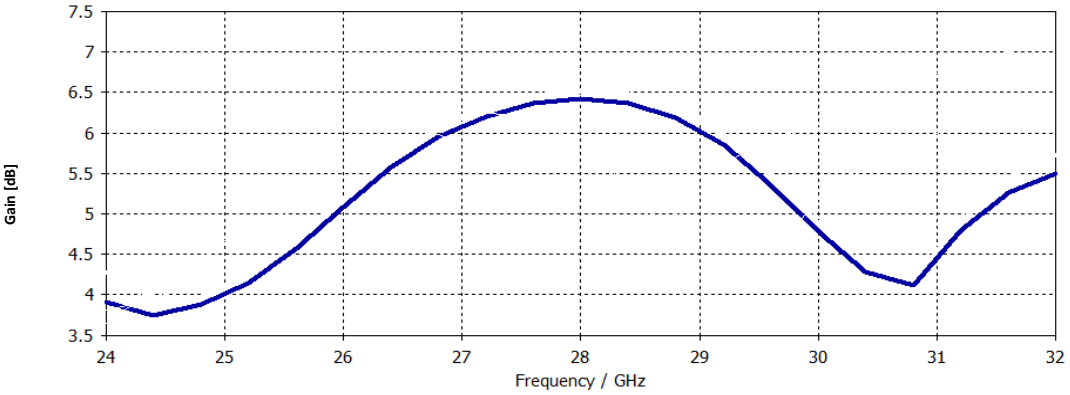

Fig.7. Gain of the design with full ground plane

Fig.8, demonstrates the surface current distributes through and on the edge of radiating element. To clarify, distinct colors obviously depicted various distributions which show how the antenna functions in several modes of operation that affect the radiation pattern of the antenna.

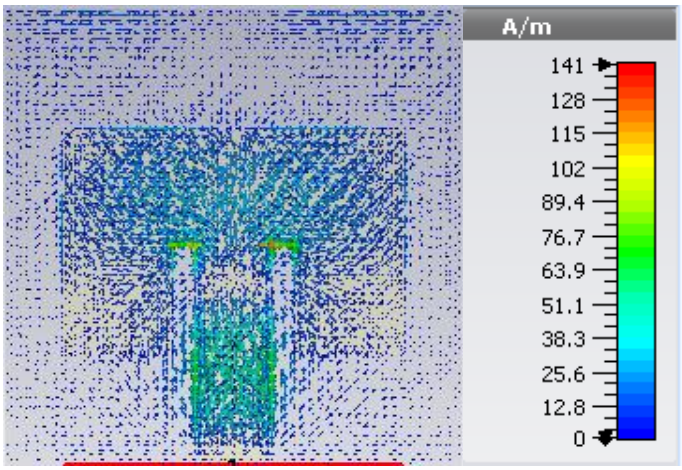

Fig.8. Surface current distribution at 28 GHz

B. Antenna design with DGS

To enhance the performance of the antenna, the ground plane is modified by etching some slots form the conducting element to increase the bandwidth, gain and system efficiency. It is also important to suppress the mutual coupling, enabling the compactness in size and multiband. Table 2, shows the last optimized design for DGS ground plane dimensions.

Table 2.Dimensions of DGS for the proposed design

Parameters	**G_0**	**G_1**	**G_2**
Dimensions (mm)	$0.5\lambda_0$	$1.67\lambda_0$	$0.15\lambda_0$

The optimized structure results in a broadband antenna with bandwidth of 13.5 GHz lying between 22.78 GHz and 35.37 GHz as shown in fig.9. Therefore, this optimized design supports majority of 5G services and supports antenna compactness. The optimized structure has two resonant frequencies at 24.07 GHz and 33.88 GHz with return losses S_{11} of about -35dB, and -33dB respectively.

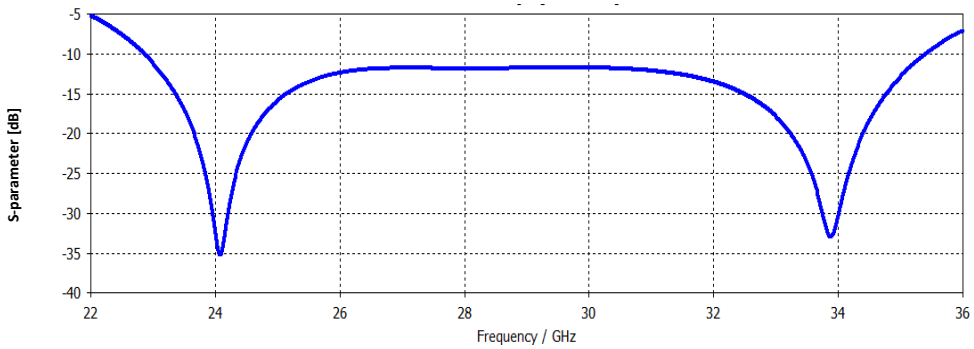

Fig. 9. Simulated S_{11} for the proposed antenna with DGS

Fig.10, illustrates the gain of the element, which provides about 6.4 dBi at frequency of 24.07 GHz, and approximately 4.5 dBi at 33.88 GHz.

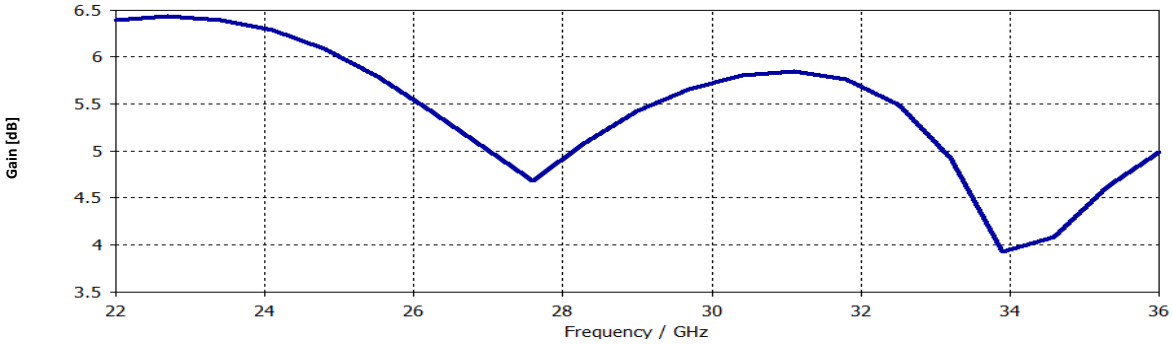

Fig. 10. Simulated S_{11} for the proposed antenna with DGS

For this sub-section, two elements of antenna array is designed and simulated, it is preferable to increase the antenna elements for the purpose of increasing the directivity and deliver more data rates. This is the concept of MIMO techniques, where more antennas are deployed at both sides of transmitter and receiver, to speed up more date rate as well as enhance the spectral efficiency; however, this may lead to both increase in antenna size and create the mutual coupling (MC) among the antenna elements . The MC appears when the excited port flow a large amount of surface current or due to surface waves. In this case there are two techniques to considerably reduce the MC either by positioning the antenna elements far by $\lambda_0/2$ between the neighboring elements or use one of the decoupling techniques to null out unwanted radiation. Fig.11, shows the design of two elements spaced by $\lambda_0/2$.

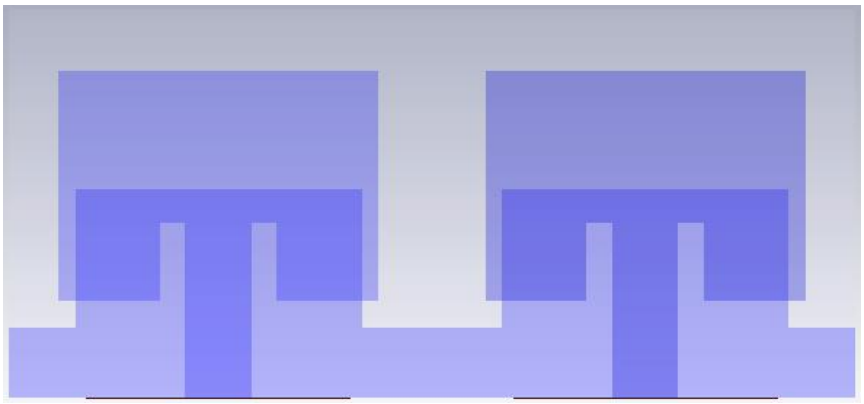

Fig.11. Design of two elements array with $\lambda_0/2$ space in between

This structure results in a bandwidth of 12.7GHz, resonating at two frequencies of 24 GHz and 33.9 GHz with return loss of both S_{11} and S_{22} of closely identical results of 28dBi and 92.8 dBi respectively. This structure provides an isolation exhibiting between -22dBi and -29 dBi over the range of the operating bandwidth. This isolation provides an envelope correlation coefficient (ECC) is less than 0.0006 with diversity gain (DG) of 10.

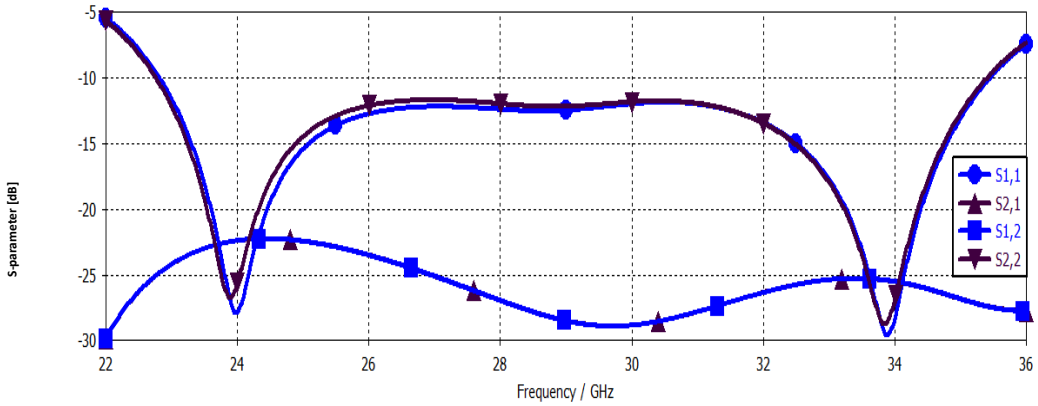

Fig. 12. Simulated S_{ij} for the proposed array design

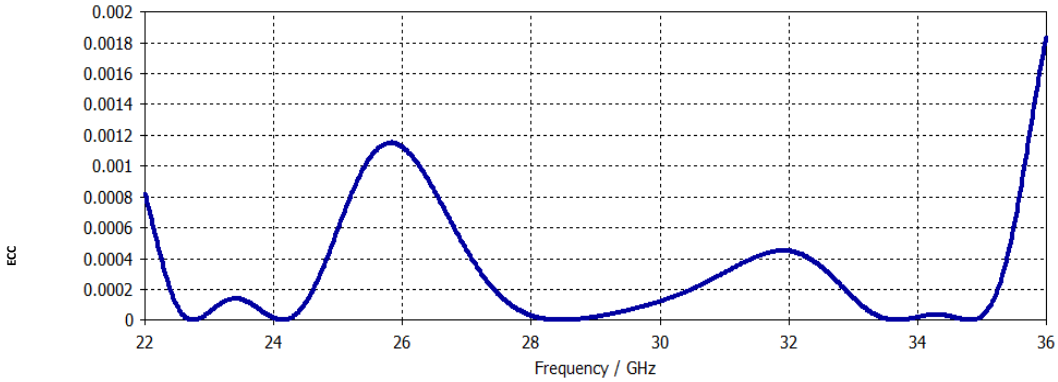

Fig. 13. Simulated ECC for the proposed array design

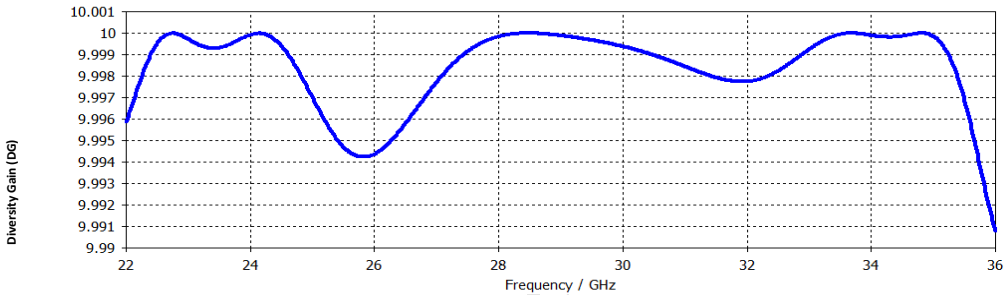

Fig. 14. Simulated $\boldsymbol{DG}$ for the proposed array design

The proposed antenna holds higher isolation, however, $\lambda_0/2$ is the minimum typical distance between the elements to ensure decoupling between neighboring elements, and this cannot support the antenna compactness and may increase the size of the antenna for multi-elements MIMO antennas.

This design is modified by reducing the space between the two active elements to be set $\lambda_{eff}/3$, where λ_{eff} is the effective wavelength with $\lambda_{eff} = \lambda_0/\sqrt{\varepsilon_{eff}}$, where ε_{eff} is the effective dielectric constant. This modification resonates at two frequencies, 24.85GHz with identical return loss of both S_{11} and S_{22} for approximately -84.07 dBi, and 34.15 GHz with return loss of -28 dBi. It also results in an isolation of -15dBi at the first resonant frequency and -23 dBi for the second resonant frequency as shown in fig.15. The ECC between the active elements in this design is higher than the design with spacing of $\lambda/2$ as demonstrated in fig.16, with diversity gain (DG) reaches to 10 as in fig.17.

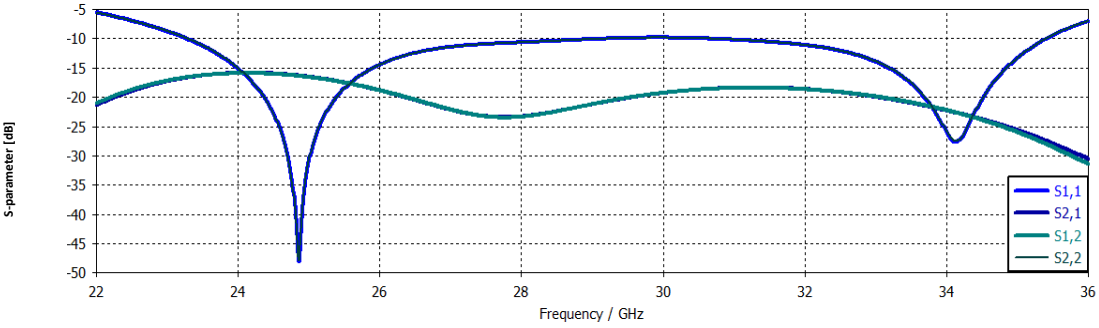

Fig. 15. Simulated $\boldsymbol{S_{ij}}$ for the proposed array design with space of $\mathbf{0.3\lambda_{eff}}$

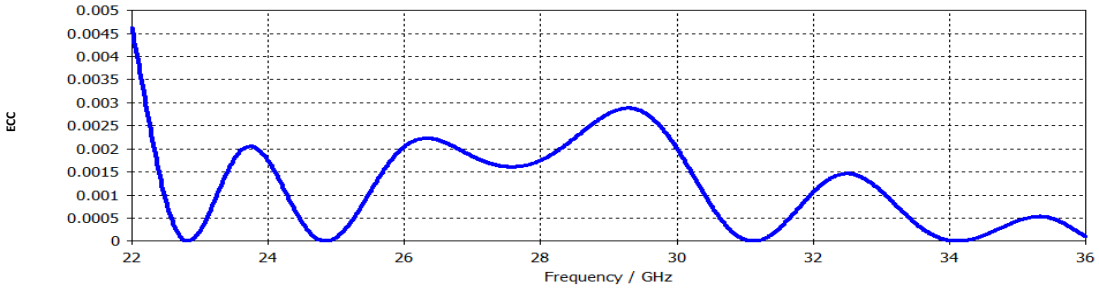

Fig. 16. Simulated $\boldsymbol{ECC}$ for the proposed array design with space of 0.3 $\lambda_{\mathbf{eff}}$

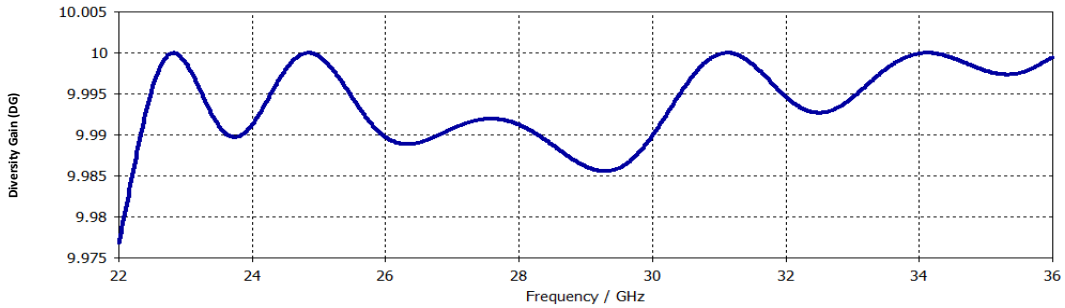

Fig. 17. Simulated $\boldsymbol{DG}$ for the proposed array design with space of 0.3 $\lambda_{\mathbf{eff}}$

Fig.18, illustrates the polar radiation pattern of the design across distinct resonant frequencies at 24.85 GHz and 34.15 GHz, for both scenarios, the radiation pattern exhibits as directional patterns.

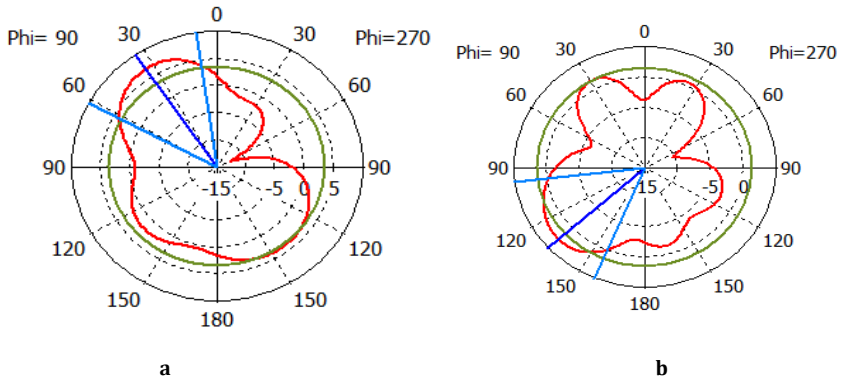

Fig.18. Far-field radiation pattern at both frequencies of (a) 24.85 GHz and (b) 34.15 GHz

D. *Design of Two antenna elements with parasitic decoupling structure*

In fig. 19, the constructed antenna is modified by inserting a decoupling element with a shape of inverted U-slap. It is used to suppress or reduce the effect of the mutual coupling.

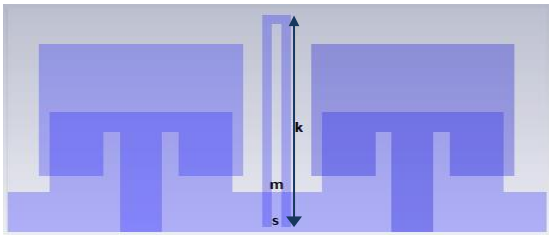

Fig.19. Design of two elements array with parasitic element

The decoupling element has dimension of outer length (k) = $0.59\lambda_0\ mm$, outer width (m) = $0.1\lambda_0\ mm$, the inner length and inner width have the values of $0.55\lambda\ mm$, and $0.33\lambda_0\ mm$ respectively. Because the active elements are symmetrically positioned on the substrate with a distance $0.3\lambda_{eff}$ and developed with a decoupling parasitic element, the results of the return loss show better performance in term of isolation. The mutual coupling reaches less than -39 dBi at the resonant frequency of 25.561 GHz with an operating bandwidth of 6.8 lying between 24.43 GHz and 31.24 GHz. The mutual coupling is also reduced to about -26 dBi at the second resonant frequency of 34.401GHz with operating bandwidth of 3.4 GHz as illustrated in fig.20. This design results in a considerable reduction in ECC to get 0.002 with 10 of diversity gain over the given range of frequencies as in fig.21 and fig.22.

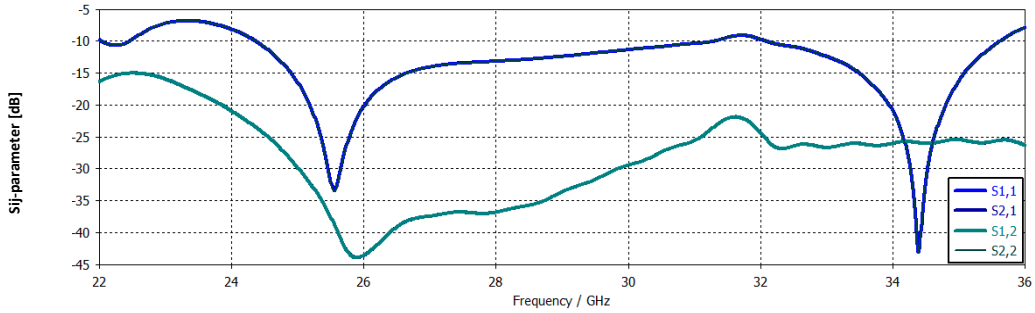

Fig. 20. Simulated $\boldsymbol{S_{ij}}$ for the design with parasitic element

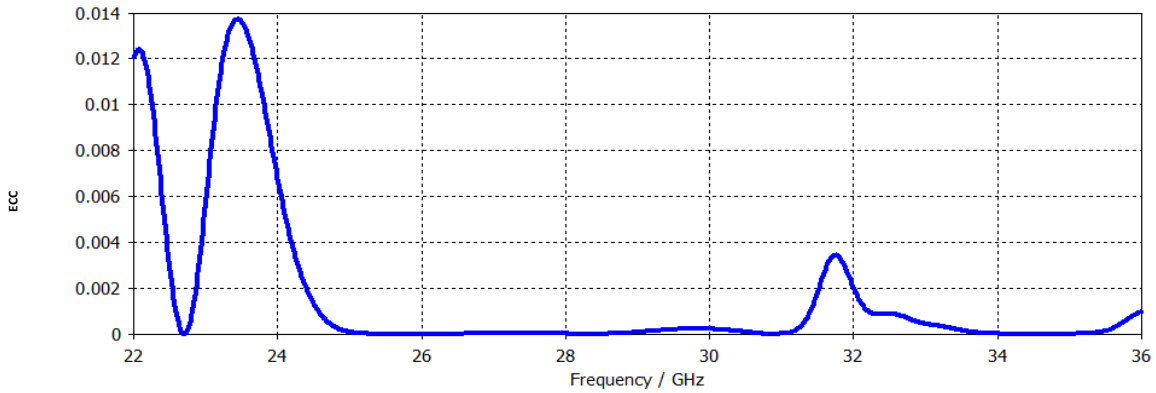

Fig. 21. Simulated $\boldsymbol{ECC}$ for the design with parasitic element

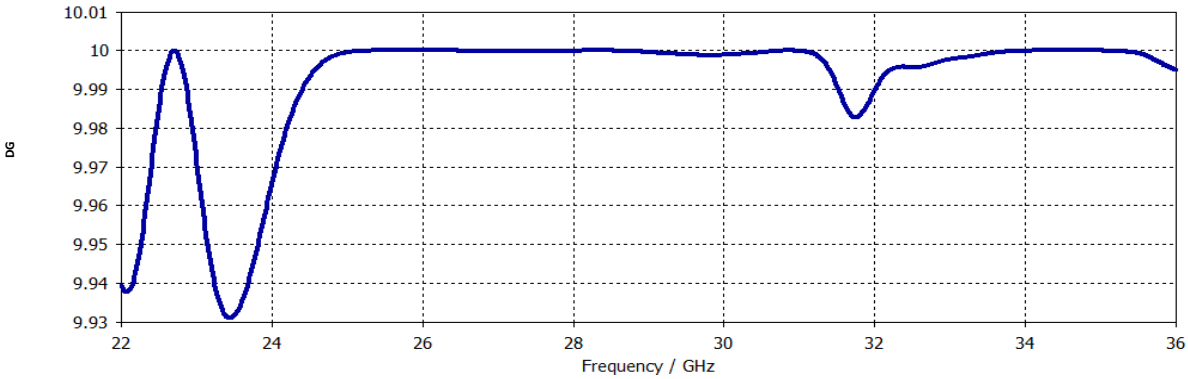

Fig. 22. Simulated ***DG*** for the design with parasitic element

The simulated results provide that this design reaches an efficiency of up to 83.5 % over the operating bandwidth as demonstrated in fig 23. In Fig 24, the radiation pattern is simulated and results in a directional radiation patter at frequencies of 25.561 GHz and 34.401GHz

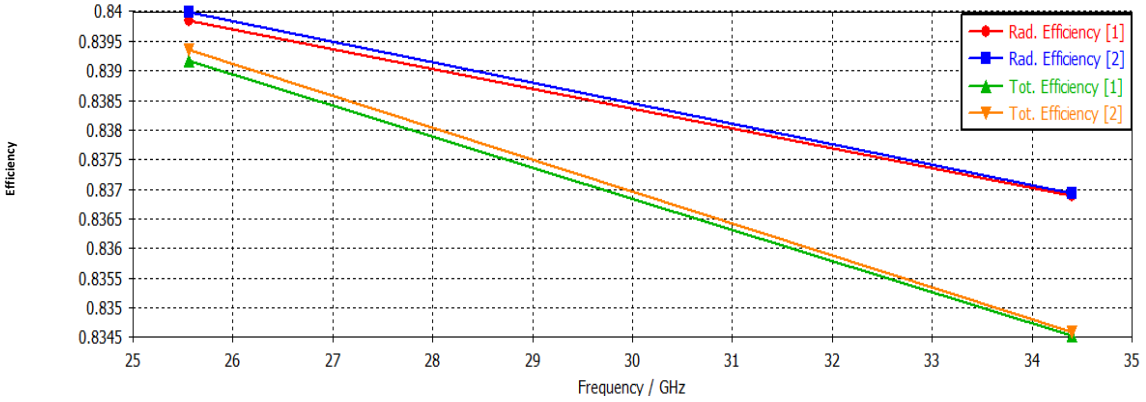

Fig. 23. Radiation efficiency for the design with parasitic element

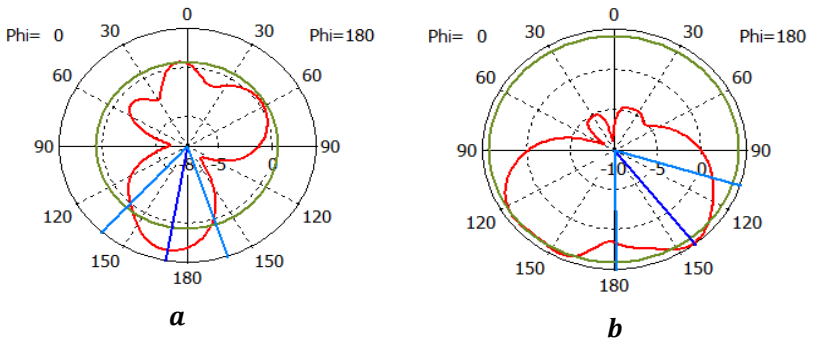

Fig. 24. Far-field radiation pattern for the design with parasitic element at (a) 25.561 GHz and (b) 34.401GHz

Table 3, represents the comparison of the proposed design with other designs of the transparent antenna in terms of size, bandwidth, modification techniques, gain, efficiency. The comparison also includes the isolation, ECC and DG and types of technique used for decoupling.

Ref	Size (mm^2)	No.of elements	BW (GHz)	Rad. efficiency (%)	Transparent	Substrate	Isolation	ECC	DG
[25]	$105x105$	2	2.23-2.46 (0.23)	≈74	yes	Plaxiglas	>12 dB	< 0.002	9.95
[26]	$24x20$	4	24.10-27.18 (3.08) 33-44.13 (10.13)	≈ 75	yes	Plaxiglas	>16 dB	< 0.1	>9.5
[27]	$26x28$	2	2.9-29.2 (26.3)	≈ 90	yes	Plaxiglas	---	< 0.002	8.1
[28]	$70x35.5$	4	1.6-19.2 (17.6)	≈ 82	yes	Wired MM	25dB	< 0.002	9.95
This work	$22.5x10$	2	24.43-31.24 (6.8) 32.18-35.95 (3.4)	≈ 83.5	Yes	Plaxiglas	>39 dB >26 dB	< 0.002	9.99

The distribution of surface current for the proposed MIMO antenna is shown in fig 25. Both designs with and without decoupling element antennas attains the maximum current intensity around their separate radiating elements which results in the higher isolation for using decoupling structure element between neighboring antennas than that without decoupling element.

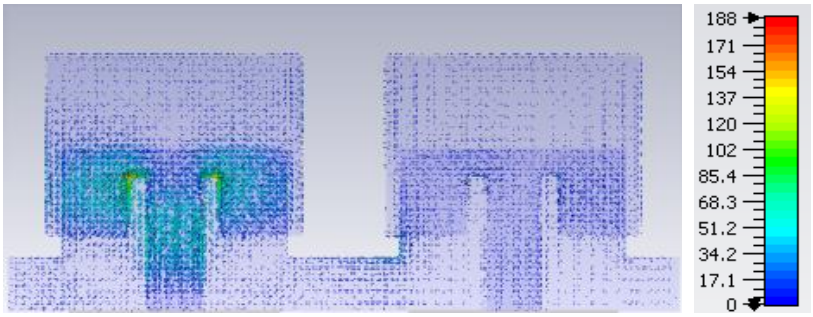

a

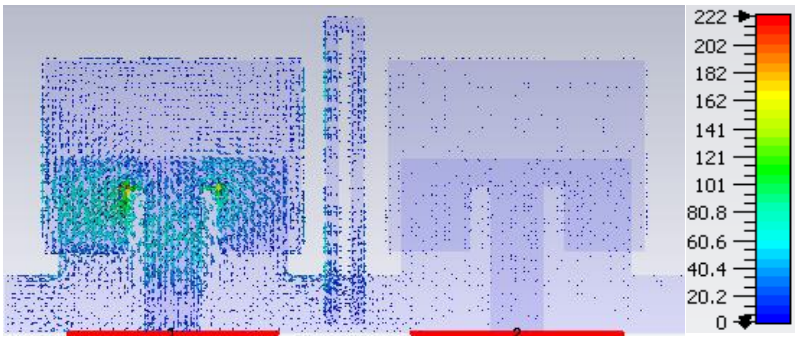

b

Fig. 25. Simulated surface current distribution for the design (a) without parasitic element,(b) with parasitic element

IV. CONCLUION

To conclude, a transparent antenna with compactness in size is designed and investigated using CST MW. The design consists of a transparent conductive material mounted on a transparent substrate made of Plexiglas. The antenna is initially designed with full ground plane to work at 28GHz, to result in impedance bandwidth of 6.43% and return loss of -43 dB. For bandwidth enhancement, it is desirable to modify the ground plane with DGS. This modification provides an achievable bandwidth and gain of 13.5 GHz and 6.5 dB respectively, with directional radiation pattern. To support more mm-wave applications, the design is extended to simulate two antennas with a parasitic element inserted in between for decoupling the unwanted waves. The outcome demonstrates that, the isolation between elements is more acceptable to have a result of ECC about 0.002 with diversity gain of 10. According to the results, the design exhibits better efficiency reaching about 85%, with current distribution has maximum current intensity around the feeding of the antenna. Therefore, the design is more suitable for 5G wireless communications and beyond.

REFERENCES

[1] Desai, Arpan, Trushit Upadhyaya, and Riki Patel. "Compact wideband transparent antenna for 5G communication systems." Microwave and Optical Technology Letters 61.3: 781-786, 2019.

[2] Yang, Qi, Hongqiang Wang, and Xin Peng. "Performance-constrained multi-objective optimization of antennas for miniaturization design." Scientific Reports 14.1: 21497, 2024.

[3] Jain, Pritesh Kumar, and Sandeep Kumar Jain. "Antenna design for IoT and 5G applications." Array and Wearable Antennas: Design, Optimization, and Applications: 59, 2024.

[4] Abdullah, Abdulati Ibrahim O., Abubaker M. Algatlawi, and Braika Alameen. "Decoupling of Compact MIMO Antennas Using Parasitic Element and Electromagnetic Band Gap Structure." 2023 IEEE 3rd International Maghreb Meeting of the Conference on Sciences and Techniques of Automatic Control and Computer Engineering (MI-STA). IEEE, 2023.

[5] Algatlawi, Abubaker M., and Abdulati IO Abdullah. "Mutual Coupling Supression Techniques Used for compact 5G MIMO Antennas." 2024 IEEE 4th International Maghreb Meeting of the Conference on Sciences and Techniques of Automatic Control and Computer Engineering (MI-STA). IEEE, 2024.

[6] Iqbal, Javed, et al. "Low-profile miniaturized circularly polarized MIMO DRA with diagonal technique for 5G Sub-6 GHz and improved mutual coupling suppression." International Journal of Microwave and Wireless Technologies: 1-11, 2025.

[7] Dominguez, Bernardo, et al. "Optically Transparent Antennas for 5G and Beyond: A Review." Electronics 14.8 : 1616, 2025.

[8] Roy, Avijit, et al. "Tungsten disulfide based wearable antenna in terahertz band for sixth generation applications." TELKOMNIKA (Telecommunication Computing Electronics and Control) 22.3: 545-555, 2024.

[9] Eralp, Mehmet Emre. Analysis and design of highly transparent and efficient antenna. MS thesis. Middle East Technical University, 2025.

[10] Moltchanov, Dmitri, et al. "A tutorial on mathematical modeling of 5G/6G millimeter wave and terahertz cellular systems." IEEE Communications Surveys & Tutorials 24.2 (2022): 1072-1116.

[11] Azizi, Sanae, et al. "Design of transparent antenna for 5G wireless applications." Proceedings. Vol. 63. No. 1. MDPI, 2020.

[12] Eralp, Mehmet Emre, Ozlem Aydin Civi, and Reyhan Baktur. "Highly Transparent and Efficient Flexible Antenna for Vehicle-to-Everything (V2X) Applications." 2024 18th European Conference on Antennas and Propagation (EuCAP). IEEE, 2024.

[13] Chishti, Abdul Rehman, et al. "Optically transparent antennas: A review of the state-of-the-art, innovative solutions and future trends." Applied Sciences 13.1: 210,2022.

[14] Eralp, M. Emre, et al. "Transparent Conductive Nanowire Antennas-Material Preparation, Characterization, and Notes on Antenna Design." 2024 IEEE International Symposium on Antennas and Propagation and INC/USNC-URSI Radio Science Meeting (AP-S/INC-USNC-URSI). IEEE, 2024.

[15] Tariq, S.; Naqvi, S.I.; Hussain, N.; Amin, Y. A metasurface-based MIMO antenna for 5G millimeter-wave applications. IEEE Access , 9, 51805–51817, 2021.

[16] Islam, Tanvir, et al. "Mutual coupling reduction in compact MIMO antenna operating on 28 GHz by using novel decoupling structure." Micromachines 14.11: 2065 ,2023.

[17] Nahin, Kamal Hossain, et al. "Performance prediction and optimization of a high-efficiency tessellated diamond fractal MIMO antenna for terahertz 6G communication using machine learning approaches." Scientific Reports 15.1: 4215, 2025.

[18] Abdelsalam, Aya E., et al. "Analysis on Different Decoupling Methods for MIMO Antenna in Ultra-Wide Band Applications: A Review." Suez Canal Engineering, Energy and Environmental Science 3.1: 26-42, 2025.

[19] Vu, Son, and Hung Luyen. "Design of Matching and Decoupling Networks with Radiation Pattern Control for Two-Element Antenna Arrays." IEEE Open Journal of Antennas and Propagation, 2025.

[20] Ghawbar, Fayad, et al. "Highly Self-Isolated 12-MIMO Antenna Elements for 5G Mobile Applications." Electronics 14.7: 1424, 2025.
[21] Muttair, Karrar Shakir, Oras Ahmed Shareef, and Hazeem Baqir Taher. "A Compact MIMO Antenna with High Efficiency for 6G Communications." Engineering Letters 33.4, 2025.
[22] Haritha, T., et al. "High-Gain Radiating Sun-Shaped Silicon-Based Wideband with Defected Ground structured Dual-Port MIMO Antenna Operating at 3.6 THz for 6G Terahertz Applications." Nano Communication Networks (2025): 100572.
[23] Patel, Arpita, et al. "Enhanced isolation in aperture fed dielectric resonator MIMO antennas for 5G Sub 6 GHz applications." Scientific Reports 15.1: 10653, 2025.
[24] Chemkha, Hichem, and Afif Belkacem. "Design of new inset fed rectangular microstrip patch antenna with improved fundamental parameters." 2020 IEEE International Conference on Design & Test of Integrated Micro & Nano-Systems (DTS). IEEE, 2020.
[25] Desai, Arpan, et al. "Dual band transparent antenna for wireless MIMO system applications." Microwave and Optical Technology Letters 61.7: 1845-1856, 2019.
[26] Desai, Arpan, et al. "Compact wideband four element optically transparent MIMO antenna for mm-wave 5G applications." Ieee Access 8 : 194206-194217, 2020.
[27] Rohaninezhad, Mohammadreza, et al. "Design and fabrication of a super-wideband transparent antenna implanted on a solar cell substrate." Scientific Reports 13.1: 9977, 2023.

AUTHORS' BIOGRAPHY

Abdulati I. Abdullah received the BSc degree in Electrical and Electronic Engineering from Azzaytuna University, Libya in 2007, and MSc degree in Data Communications form The University of Sheffield, UK in 2014. He is working as a lecturer with Department of Electric and Electronic Engineering at Azzaytuna University, Tarhunah, Libya since 2015. He is ranked as an assistant Professor since June 2023. He is serving different conferences and journals as a reviewer, and a regular reviewer with some IEEE conferences. His research interest includes: 5G wireless communications and beyond, mm-wave antennas and spatial modulation. He has published many articles in Scopus.

Ahmed H. Elshoshi received the BSc degree in Electrical and Electronic Engineering from Al-Mergeb University, Libya in 2006, and MSc degree in computing and Electronic Engineering, University of Huddersfield, UK in 2015. He is working as a full time lecturer with Department of Electric Engineering, Higher Institute of Engineering Technology, Tripoli, Libya since 2015. His research of interest includes: 5G wireless communications and beyond, mm-wave antennas